Chemical Engineering Journal 164 (2010) 56–62

Contents lists available at ScienceDirect

Chemical Engineering Journal

journal homepage: www.elsevier.com/locate/cej

Removal of Cu^{2+} from aqueous solution by adsorption in a fixed bed column and Neural Network Modelling

Ensar Oguz*, Muhammed Ersoy

Atatürk University, Environmental Engineering Department, 25240 Erzurum, Turkey

ARTICLE INFO

Article history:
Received 3 June 2010
Received in revised form 6 August 2010
Accepted 10 August 2010

Keywords:
Fixed bed column
Copper ions
Sunflower
Neural Network
Adsorbent capacity

ABSTRACT

Adsorption potential of shells of *Sunflower* to remove Cu^{2+} ions from aqueous solution was investigated using a fixed-bed adsorption column. The effects of inlet $Cu_o{}^{2+}$ concentration (20–60 mg/L), feed flow rate (9–21 mL/min) and bed height (5–15 cm), initial solution pH (3–5.6) and particle size (0.25–0.5, 0.5–1 and 1–2 mm) on the breakthrough characteristics of the adsorption system were investigated. The adsorption capacities of the adsorbent at different particle sizes (0.25–0.5, 0.5–1, 1–2 mm) were determined as 17.26, 7.36 and 5.48 mg/g, respectively. The highest experimental and theoretical bed capacities were obtained to be 25.95 and 26.22 mg/g at inlet $Cu_o{}^{2+}$ concentration of 60 mg/L, bed height of 5 cm and flow rate of 5 mL/min, pH of 5.6 and particle size of 0.25–0.5 mm. A relationship between the predicted and observed data was conducted. The ANN model yielded determination coefficient of 0.986 and root mean square error of 0.018. The results indicated that *Sunflower* waste is a suitable adsorbent for the removal of Cu^{2+} ions from aqueous solution.

1. Introduction

Human activities, such as the discharge of industrial wastes and mining operations, have resulted in the accumulation of metals in the environment [1,2]. Some metals such as Ca, Co, Cr, Cu, Zn, Fe, K, Mg, Mn, Na and Ni are essential micro-nutrients for most living organisms. One of the most important functions of the micro-nutrients is their role in metalloenzymes. However, when the concentrations of beneficial metals, for instance, copper or zinc in the environment are excessively high they can become toxic to these microorganisms and human [3].

The uptake of heavy metal ions from wastewater has attracted a great attention in recent years for global awareness of the underlying detriment of toxic metals in the environment. Application of traditional processes for the uptake of heavy metals has enormous cost, and they cause further environment damage because of the continuous input of chemicals. Hence, easy, effective, economic and ecofriendly techniques are required for fine-tuning of effluent wastewater treatment [4].

Biosorption of metals by biomass has been much explored in recent years. Different form of inexpensive, non-living plant material such as rice husk [5], sawdust [6] and pine bark and canola meal [7–10] have been widely investigated as potential adsorbents for heavy metals.

The biosorption capacity parameter obtained from a batch experiment is useful in providing information about effectiveness of heavy metal-biosorbent system. However, the data obtained under batch conditions are generally not applicable to most treatment system where contact time is not sufficient long for the attainment of equilibrium. Hence, there is a need to perform equilibrium studies using columns [11].

In practice the column type continuous flow operations which are more useful in large-scale wastewater treatment have distinct advantages over batch treatment. It is simple to operate, attains a high yield and it can be easily scaled up from a laboratory-scale procedure. The stages in the separation process can also be automated and high degrees of purification can often be achieved in a single step process. A packed bed is also an effective process for cyclic sorption/desorption, as it makes the best use of the concentration difference known to be a driving force for biosorption and allows more efficient utilization of the sorbent capacity and results in a better quality of the effluent. A large volume of wastewater can be continuously treated using a defined quantity of biosorbent in the column [12–15].

The aim of this study is to remove Cu^{2+} ions by the shells of *Sunflower* from aqueous solution using a fixed-bed adsorption column. We here have investigated the effects of flow rate, pH value, influent concentration, bed depth and particle size on metal uptake by the shells of *Sunflower* in a fixed bed column. A model based on an artificial neural network (ANN) has been constructed to model Cu^{2+} concentration removed from aqueous solution as a function of emperical parameters.

* Corresponding author. Tel.: +90 442 231 4601.
E-mail address: eoguz@atauni.edu.tr (E. Oguz).

1385-8947/$ – see front matter © 2010 Elsevier B.V. All rights reserved.
doi:10.1016/j.cej.2010.08.016

2. Materials and methods

2.1. Biosorbent preparation

Shells of *Sunflower* were used in this study. The shells of *Sunflower* were gathered in 2009. Fresh shells of *Sunflower* were dried in outdoors for 72 h and cut into small pieces, ground in a blender to granulate and get it sieved to separate to different particle sizes (0.25–0.5, 0.5–1 and 1–2 mm).

The surface area of the shells of *Sunflower* was measured by BET method at 77 K using a Quantachrome QS-17 model apparatus [16]. The surface area of the shells of Sunflower was determined as 1.82 m^2/g.

Cu^{2+} solutions were prepared by diluting 400 ppm of $CuSO_4{\cdot}5H_2O$ (Merck) stock solution with deionized water to a desired concentration range between 20 and 60 mg/L. The initial concentration of the $Cu_o{}^{2+}$ in the solution and samples after biosorption process was complexometrically determined [17].

2.2. Column experiments

Continuous flow adsorption experiments were conducted in teflon columns of 1 cm i.d. and 5, 10 and 15 cm heights as seen from Fig. 1. A known quantity of adsorbent was placed in the column to receive the desired bed height. Cu^{2+} solution having an initial concentration of 40 mg/L was pumped upward through the column at a desired flow rate by a peristaltic pump. Samples were collected from the exit of the column at different intervals and analyzed for Cu^{2+} concentration. Operation of the column was stopped when the effluent Cu^{2+} concentration equals approximately influent $Cu_o{}^{2+}$ concentration.

The total quantity of metal adsorbated in the column was calculated from the area above the breakthrough curve (outlet metal concentration versus time) multiplied by the flow rate. Dividing the metal mass by the biosorbent mass (M) leads to the uptake capacity (Q) of the biomass. The total amount of metal ions sent to the column can be calculated from Eq. (1) [18].

$$m_{total} = \frac{C_o F t_e}{1000} \quad (1)$$

where C_o is the inlet metal ion concentration (mg/L), F the volumetric flow rate (mL/min) and t_e is the exhaustion time (min). The mass transfer zone can be calculated from the difference between

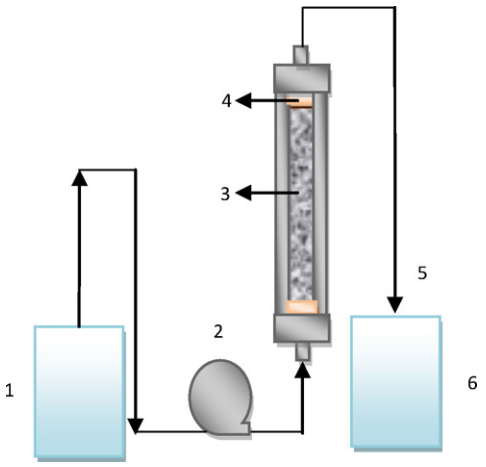

Fig. 1. Schematic diagram of experimental set up: (1) feed tank; (2) peristaltic pump; (3) fixed bed of the shells of *Sunflower*; (4) bed support; (5) sampling port measuring Cu^{2+} concentration (6) effluent collector.

column exhaustion time (t_e) and column breakthrough time (t_b). The slope of the breakthrough curve from t_b to t_e was represented by dc/dt. Total metal removal (%) with respect to flow volume can be calculated from the ratio of metal mass adsorbed (m_{ad}) to the total amount of metal ions sent to the column, given by Eq. (2) [19].

$$\text{total metal removal } (\%) = \frac{m_{ad}}{m_{total}} \times 100 \quad (2)$$

The amount of metal retained in the column depends on the influent metal concentration and can be calculated from the area above the breakthrough curve (Eq. (3)) [20].

$$q = \frac{C_o Q}{m \times 1000} \int_0^t \left(1 - \frac{C_t}{C_o}\right) dt \quad (3)$$

where q represents the amount of metal retained (mg of copper per g of adsorbent), C_t and C_o are the copper concentrations at the column effluent and influent (mg/L) respectively, Q is the flow rate (mL/min), m is the mass of adsorbent in the column (g) and t is the adsorption time (min).

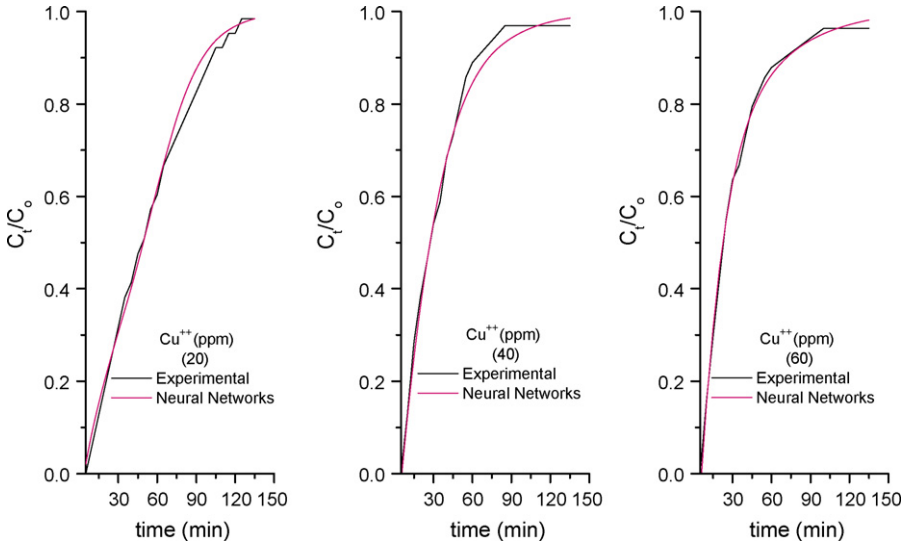

Fig. 2. Experimental and theoretical breakthrough curves of Cu^{2+} adsorption as a function of inlet Cu^{2+} concentration (T 15 °C, pH 5.6, flow rate 9 mL/min, bed depth 5 cm, particle size 0.25–0.5 mm).

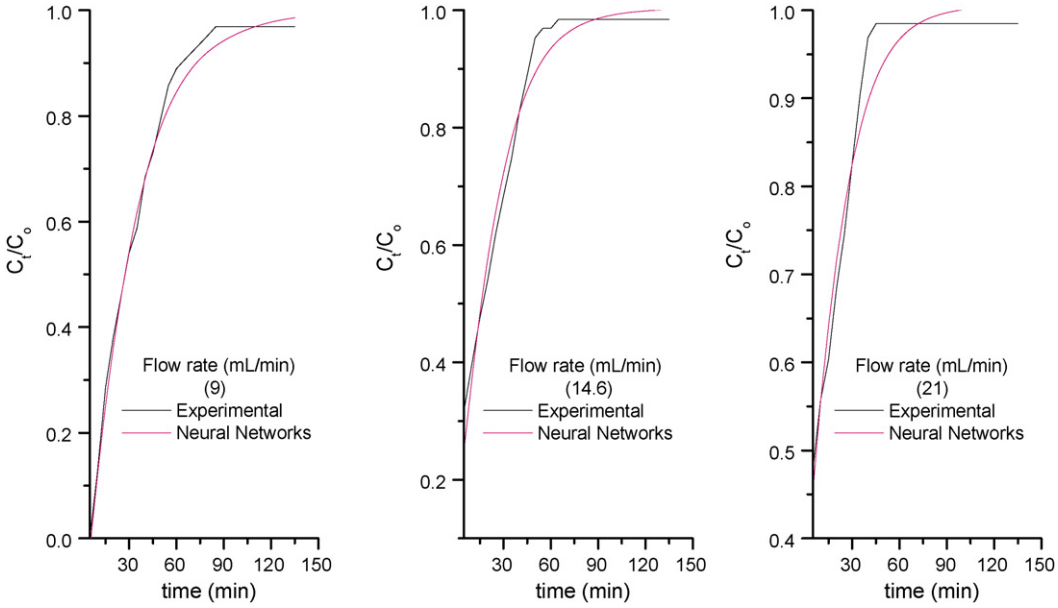

Fig. 3. Experimental and theoretical breakthrough curves of Cu^{2+} adsorption as a function of flow rate (T 15 °C, pH 5.6, Co 40 ppm, bed depth 5 cm, particle size 0.25–0.5 mm).

3. Results

3.1. The effect of experimental conditions on the breakthrough curve

The effect of influent Cu_o^{2+} concentration on the shape of the breakthrough curves was shown in Fig. 2. As shown in Fig. 2, in the interval of 50 min, the value of C_t/C_o reached 0.5, 0.79 and 0.82 when influent concentration was 20, 40 and 60 mg/L respectively.

It is illustrated in Fig. 2 that the breakthrough time decreased with the increase of influent Cu_o^{2+} concentration. At lower influent Cu_o^{2+} concentration, breakthrough curve was dispersed and breakthrough occurred slower. As influent concentration increased, sharper breakthrough curves were observed. These results demonstrate that the change of concentration gradient affects the saturation rate and breakthrough time. These results also show that the change of concentration gradient affects the saturation rate of adsorbent and breakthrough time, in other words, the diffusion process is concentration dependent. As the influent concentration increases, Cu_o^{2+} loading rate increases, so does the driving force for mass transfer, in which adsorption zone length decreases [21].

The effect of flow rate on the adsorption of Cu_o^{2+} in the fixed bed with bed depth of 5 cm was investigated. The flow rate was changed in the range of 9–21 mL/min while the concentration of Cu_o^{2+} in influent was kept constant at 40 mg/L. The adsorption breakthrough curves obtained at different flow rates are shown in Fig. 3. The obtained results show that the adsorption of Cu_o^{2+} on the shells of *Sunflower* was strongly influenced by the flow rate. All the breakthrough curves had a similar shape. The breakthrough curves shifted to the origin with increasing flow rate, and an earlier break-

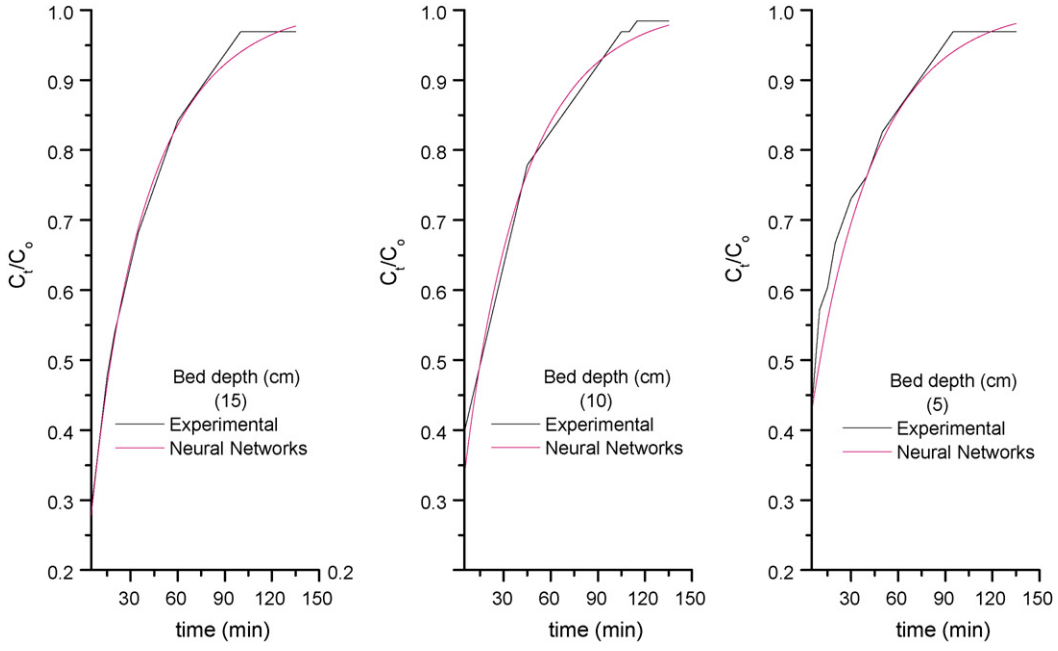

Fig. 4. Experimental and theoretical breakthrough curves of Cu^{2+} adsorption as a function of bed depth (T 15 °C, pH 5.6, Co 40 ppm, flow rate 9 mL/min, particle size 1–2 mm).

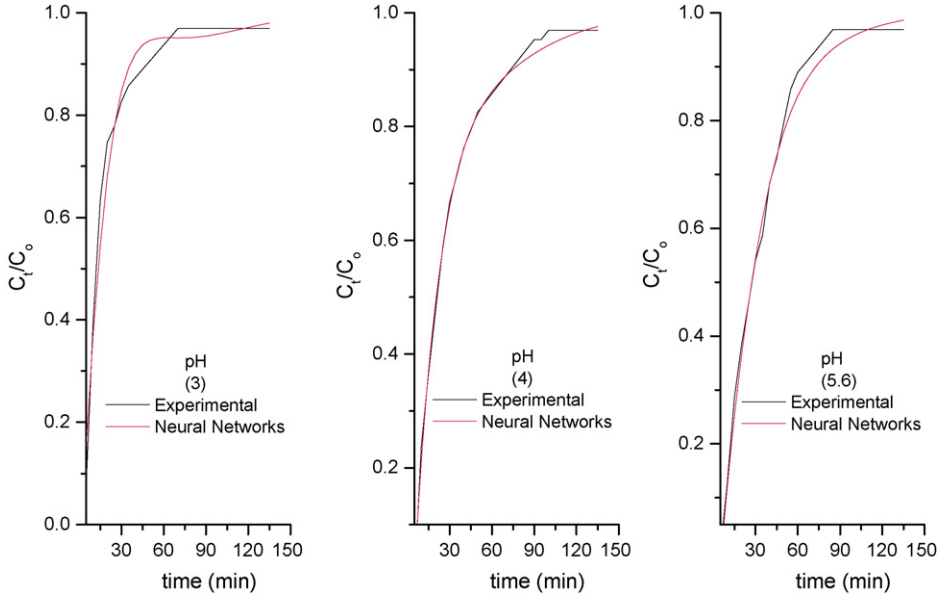

Fig. 5. Experimental and theoretical breakthrough curves of Cu^{2+} adsorption as a function of pH of solution (T 15 °C, bed depth 5 cm, Co 40 ppm, flow rate 9 mL/min, particle size 0.25–0.5 mm).

through time and saturation time were observed for a higher flow rate. Fig. 3 shows that Cu_o^{2+} concentration in the effluent increased rapidly after the breakthrough time, as the solution continued to flow, the fixed bed became saturated with Cu_o^{2+}, and Cu_o^{2+} concentration in the effluent approached the influent concentration. Both equilibrium uptake and total removal efficiency of Cu_o^{2+} decreased with increasing flow rate, and their maximum value was obtained at the lowest flow rate of 9 mL/min. As shown in Fig. 2, in the interval of 50 min, the value of C_t/C_o reached 0.91, 0.95 and 0.99 when flow rate was 9, 14.6 and 21 mL/min, respectively.

Another important parameter in the adsorption process is relevant to the bed depth. However, because of the pressure drop and the handling problems of the smaller particle size <0.5–1 mm in the column studies, the particle sizes of 1–2 mm were used to compare C_t/C_o with adsorbent capacities for the bed depths of 5, 10 and 15 cm.

The retention of metals in a fixed bed column depends, among other factors, on the quantity of adsorbent used or, on the bed depth of the column works. The adsorption performance of the shells of *Sunflower* was investigated at various bed heights of 5, 10 and 15 cm at a flow rate of 9 mL/min where inlet Cu_o^{2+} concentration was kept constant at 40 ppm. Fig. 4 shows the breakthrough profile of Cu_o^{2+} adsorption at different bed heights. For the different three bed depths used, as the bed depth increases, the quantity of the removed Cu_o^{2+} concentration increases which is also illustrated by the service time change. As shown in Fig. 4, in the interval of 50 min, the value of C_t/C_o reached 0.82, 0.79 and 0.77 when bed depth was 5, 10 and 15 cm, respectively. At the column depth with 5 cm, the adsorbent becomes saturated very quickly because saturation at the binding sites is faster.

The pH value of the solution is an important controlling parameter in the adsorption process, and the pH value of aqueous solution

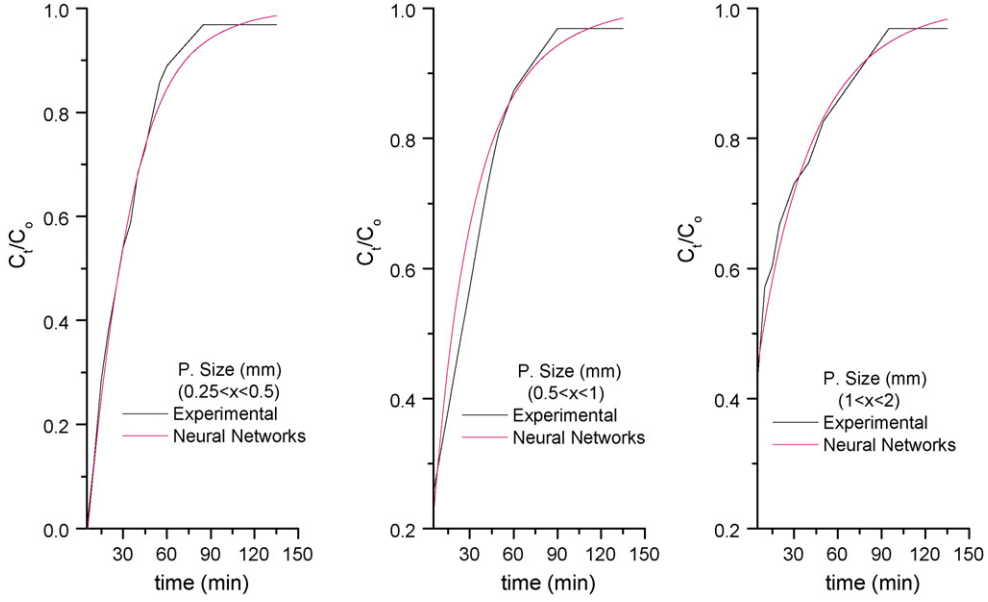

Fig. 6. Experimental and theoretical breakthrough curves of Cu^{2+} adsorption as a function of particle size (T 15 °C, bed depth 5 cm, Co 40 ppm, flow rate 9 mL/min, pH 5.6).

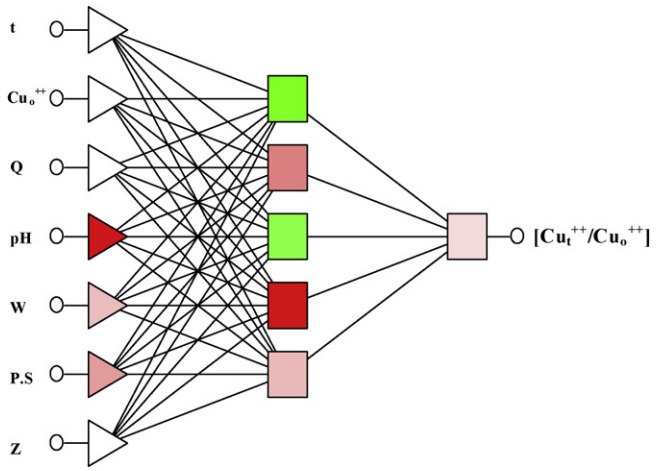

Fig. 7. The architecture of the ANNs used in this study.

has more influence to uptake Cu_o^{2+} ions in the fixed bed. It influences both the adsorbent surface metal binding sites and the metal chemistry in water. When pH of feed solution was changed from 3 to 5.6, the highest adsorbent capacity and the longest breakthrough time was achieved at pH 5.6. As shown in Fig. 5, in the interval of 50 min, the value of C_t/C_o reached 0.90, 0.82 and 0.79 when pH value of the solution was 3, 4 and 5.6, respectively. At the column depth with 5 cm, the adsorbent becomes saturated very quickly because saturation at the binding sites is faster.

The pH of the aqueous solution is also an important controlling parameter in the adsorption process [22]. In the range of pH 3–5.6, there are three species present in solution as suggested by [22]. The dominant species between pH 3 and 5.6 in the Cu^{2+} solution were Cu^{2+}, $Cu(OH)^+$ and $Cu(OH)_2$. These species are adsorbated with electrostatically interaction at the surface of the shells of *Sunflower*. As the pH decreases, the surface of *Sunflower* exhibits an increasing positive characteristic, thus breakthrough time decreased. Obviously with an increase of pH in the influent, the breakthrough curves shifted from left to right, which indicates that more metal ions can be removed.

Another important parameter in the adsorption process is related to the particle size of the adsorbent. The particle sizes were 0.25–0.5, 0.5–1 and 1–2 mm, while the bed depth, influent Cu^{2+} concentration and pH were kept constant at 5 cm, 40 mg/L and 5.6, respectively. The breakthrough curves of concerning with particle size are given in Fig. 6. An increase in the particle size appeared to increase the sharpness of the breakthrough curve. Furthermore, the adsorption capacity for the larger particle size is lower than that for smaller one. A rapid decrease in the column adsorption capacity with an increase in the particle size was observed. The clear shift of the breakthrough curve was obtained from 0.25–0.5 to 1–2 mm. This is mainly true due to the higher surface area of the smaller particle size. Thus, a higher adsorption capacity and shorter intraparticle diffusion path are expected. As shown in Fig. 6, in the interval of 50 min, the value of C_t/C_o reached 0.79, 0.81 and 0.83 when the particle size was 0.25–0.5, 0.5–1 and 1–2 mm, respectively.

Table 1
Shift and scale factors.

	Shift	Scale
t (min)	−0.038	0.007
Cu_o^{++} (mg/L)	−0.500	0.025
Q (mL/min)	−0.750	0.083
pH	−1.200	0.400
M (g)	−0.189	0.315
P.S (mm)	−0.333	0.888
Z (cm)	−0.500	0.100
Cu_t^{++} (mg/L)	0.000	1.015

4. Application of artificial neural network

A linear model is not suitable to constitute a satisfying relationship among the input variables for a biosorption process. In fact, it is reasonable to consider that such variables are not totally independent. The ANN approach seems to be completely suitable to the problems where the relations between variables are not linear and complex [23,24].

A neuron sums the product of each connection weight (w_{jk}) from a neuron (j) to the neuron (k) and, input (x_j) and the additional weight called the bias to get the value of sum for the neuron. The ith neuron has a summer that gathers its weighted input $w_{ij} \cdot p_j$ and the bias b_i to form its net input n_i, which given by Eq. (4)

$$n_i = \sum w_{ij}x_j + b_i \tag{4}$$

where w_{ij} denotes the strength of the connection from the jth input to the ith neuron, x_j is the input vector, b_i is the ith neuron bias. The sum of the weighted inputs is further transformed with a *transfer function* to get the output value. There are several transfer functions; the most common is the sigmoidal function [23–26]. To find suitable w_s and biases for each neuron, a process training is essential; it is the first step to build an ANN. Training means that the weights are corrected to produce prespecified ("correct", known from experiments) target values, and the training requires sets of pairs (X_S, Y_S) for input: the actual input into the network is a vector (X_S), and the corresponding target is labelled (Y_S) after successful

Table 2
Connection weights and biases.

Bias	2.1	2.2	2.3	2.4	2.5	3.1
			b_1			b_2
	−0.913	0.297	0.763	−0.001	0.284	1.347
			w_1			
1.1	3.257	−1.396	3.869	−2.933	−1.574	
1.2	−0.675	−1.006	2.468	0.751	0.262	
1.3	0.458	−0.442	0.502	−1.358	−1.831	
1.4	0.387	−2.189	−0.894	−0.845	−0.515	
1.5	0.072	0.844	1.799	1.115	0.286	
1.6	0.774	−0.3909	3.194	−1.816	0.054	
1.7	−0.679	0.213	1.340	0.399	−0.137	w_2
2.1						2.902
2.2						0.874
2.3						0.298
2.4						0.859
2.5						−0.900

Table 3
Sensitivity analysis results.

	t	Cu_o^{++} (mg/L)	Q (mL/min)	pH	M (g)	P.S (mm)	Z (cm)
Rank	1	6	3	5	4	2	7
Ratio	9.650	2.165	3.220	2.236	2.655	4.434	1.278

training. When correct values of Y_S for each vector of X_S from the training set are obtained, it is hoped that the network will give correct predictions of Y for any new object of X according to the ANN model fundamentals and with the use of more data for training the network, better result would be obtained. The most utilized training method for multilayered neural network is called *back propagation* [27].

Information about errors (differences between target and predicted values) is filtered back through the system and is used to adjust the connections between the layers, thus performance improves. In the early standard algorithm, random initial set of weights was assigned to the neural network, and then by considering the input data, weights were adjusted, so the output error would be on its minimum [28]. In this study, one-layered back propagation neural network was used for modelling of the uptake of Cu^{2+} ions from aqueous solutions (Fig. 7). The input variables to the neural network are as follows: the treatment time (t), the concentration of initial Cu_o^{2+}, adsorbent dosage, pH, flow rate, bed depth and particle size. Cu_o^{2+} concentration as a function of reaction time was chosen as the experimental response or output variable. In order to model the Cu_t^{2+} concentrations with ANN, the Statistica software program was used. The coefficient of root mean square error (RMSE) is the main criterion to evaluate the performance of ANN, which is defined as follows:

$$\mathrm{RMSE} = \sqrt{\frac{(\mathrm{obs} - \mathrm{pre})^2}{n}} \quad (6)$$

Low value of the RMSE satisfies the statistical evaluation of prediction for the validation [29,30]. From Fig. 6, it can be observed that the newly constructed neural network was precise in predicting the Cu^{2+} uptake with a high correlation coefficient of 0.986. This shows that the developed Neural Network Model can be precise in predicting the removal of Cu^{2+} by the shells of *Sunflower* for the range of experimental conditions [31].

Before the network was trained, the input and the output data were normalized. The scale and shift factors used in each input and output are given in Table 1.

The weight coefficients and the biases given in Table 2 are the values obtained for the normalized data in order to determine the actual (experimental) Cu_t^{2+} concentration. An inverse transformation on this data is performed using shift and scale factors. After long training phases, the best result was obtained from the Levenberg–Marquardt algorithm.

The hyperbolic tangent function in the hidden layer and the linear activation function in the output layer were used in the model. It was observed that the optimal network was found to have seven inputs, one hidden layer with five neurons and one output layer. The optimal network architecture (7:7–5–1:1) is shown in Fig. 7.

Sensitivity analysis is a useful technique to assess the relative contribution of the input variables to the performance of a neural network by testing the neural network when each input variable is unavailable. This indicates that the input variables are considered to be the most important ones by a particular neural network. If the ratio is one or lower, the input variable has no effect on the performance of the network. Otherwise, ratios of input parameters are more than one, all input variables are meaningful. The results of the sensitivity analysis are given in Table 3.

It can be seen from Table 3 that the most important parameter that affects the removal of the Cu_t^{2+} are adsorption time, particle size (P.S), flow rate (Q), adsorbent dosage (M), pH, initial Cu_o^{2+} concentration and bed depth (Z), respectively.

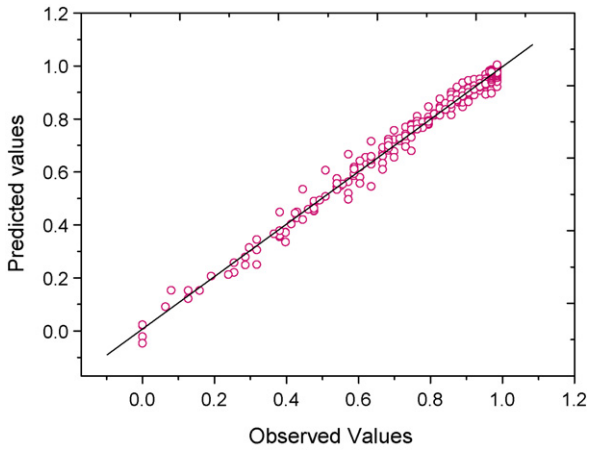

Fig. 8. The relationship between observed and theoretical values relating to general model (R^2 0.986).

Before training the network, both the input and output variables were normalized within the range of 0–1 using a minimax algorithm. The minimum and maximum of the data set were found and scaling factors were selected so that these were mapped to the desired minimum and maximum values.

The number of experimental data used in the ANN is 324 which were divided into three sections: the training set (162 data), verification set (81 data) and test set (81 data). Training algorithms do not use the verification or test sets to adjust network weights. The verification set may optionally be used to track error performance of the network to identify the best network and to stop training, if over-learning occurs. The test set is not used in training at all, and it is designed to give an independent assessment of the performance of the network when the design procedure of an entire network is completed. The assignment of the cases to the training, verification and test subsets can sometimes affect the performance of the training algorithms. In order to eliminate this drawback, the cases should be shuffled randomly between subsets. The cases can be left in their original order or grouped together in the subsets. In this model, the cases were shuffled randomly between the subsets (training, test and verification).

The general model obtained from the ANN belonging to all of the parameters (adsorption time, Cu_o^{++} concentration, adsorbent dosage, adsorbent particle size, agitation rate, pH) was given in Fig. 8.

5. Conclusion

The shells of *Sunflower* were used to define the experimental and theoretical adsorbent capacities in a fixed bed column. The C_t/C_o, q_{exp} and q_{cal} are a function of the adsorption time, adsorbent dosage, adsorbate concentration, adsorbent particle size, pH and bed depth. An artificial Neural Network Modelling has been used to investigate relation between the cause and effect in the adsorption studies of Cu^{2+} ions. The ANN model could describe the behavior of the adsorption with the adopted experimental conditions. A simulation based on the ANN model has then been performed in order to

estimate the behavior of the system under different conditions. The model based on the ANN has predicted the concentrations of Cu_t^{2+} uptake in a fixed bed column during adsorption time. A relationship between predicted and observed data has been constructed. In the ANN model, the value of root mean square error was obtained to be 0.41. According to the sensitivity analysis results, the most important parameters affecting the adsorbent capacity were found to be as adsorption time, particle size, flow rate, adsorbent dosage, pH, initial Cu_o^{2+} concentration and bed depth.

Acknowledgements

Authors are grateful the research council of Atatürk University to provide financial support under the project no: 2008/149.

References

[1] X.C. Chen, Y.P. Wang, Q. Lin, J.Y. Shi, W.X. Wu, Y.X. Chen, Biosorption of copper(II) and zinc(II) from aqueous solution by Pseudomonas putida CZ1, Colloids Surf. B: Biointerfaces 46 (2005) 101–107.
[2] C.K. Wong, Bull. Environ. Contam. Toxicol. 50 (1993) 633.
[3] G.M. Gadd, Fungal response towards heavy metals, in: R.A. Herbert, G.A. Codd (Eds.), Microbes in Extreme Environments, Academic Press, London, 1986, pp. 83–110.
[4] R. Han, J. Zhang, W. Zou, H. Xiao, J. Shi, H. Liu, Biosorption of copper (II) and lead (II) from aqueous solution by chaff in a fixed-bed column, J. Hazard. Mater. B133 (2006) 262–268.
[5] N. Khalid, A. Rahman, S. Ahmad, S.N. Kiani, J. Ahmad, Adsorption of cadmium from aqueous solutions on rice husk, Plant Soil 197 (1998) 71–78.
[6] Z.R. Holan, B. Volesky, Accumulation of cadmium, lead and nickel by fungal and wood biosorbents, Appl. Biochem. Biotechnol. 53 (1995) 133–146.
[7] S Al-Asheh, Z. Duvnjuk, Binary metal sorption by pine bark: study of equilibria and mechanisms, Separ.Sci. Technol. 133 (9) (1998) 1303–1329.
[8] S. Al-Asheh, G. Lamarche, Z. Duvnjuk, Investigation of copper sorption using plant materials, Water Qual. Res. J. Can. 33 (1) (1998) 167–183.
[9] H. Ucun, Y.K. Bayhan, Y. Kaya, A. Cakici, O.F. Algur, Biosorbtion of chromium (VI) from aqueous solution by cone biomas of Pinus sylvestris, Biores. Technol. 85 (2002) 155–158.
[10] Y. Nuhoglu, E. Oguz, Removal of copper(II) from aqueous solutions by biosorption on the cone biomass of Thuja orientalis, Process Biochem. 38 (2003) 1627–1631.
[11] H. Runping, W. Yuanfeng, Y. Weihong, Z. Weihua, S. Jie, L. Hongmin, Biosorption of methylene blue from aqueous solution by rice husk in a fixed-bed column, J. Hazard. Mater. 141 (2007) 713–718.
[12] E. Valdman, L. Erijman, F.L.P. Pessoa, S.G.F. Leite, Continuous biosorption of Cu and Zn by immobilized waste biomass *Sargassum* sp, Process Biochem. 36 (2001) 869–873.
[13] Z. Zulfadhly, M.D. Mashitah, S. Bhatia, Heavy metals removal in fixed-bed column by the macro fungus *Pycnoporus sanguineus*, Environ. Pollut. 112 (2001) 463–470.
[14] T. Robinson, B. Chandran, G.S. Naidu, P. Nigam, Studies on the removal of dyes from a synthetic textile effluent using barley husk in static-bath and in a continuous flow packed-bed reactor, Biores. Technol. 85 (2002) 43–49.
[15] F. Rozada, L.F. Calvo, A.I. Garc'la, J. Mart'In-Villacorta, M. Otero, Dye adsorption by sewage sludge-based activated carbons in batch and fixed bed systems, Biores. Technol. 87 (2003) 221–230.
[16] S. Brunauer, P. Emmett, J. Am. Chem. Soc. 60 (1938) 309–319.
[17] H. Gülensoy, Komplexometrinin esasları ve komplexsometrik titrasyonlar, Fatih Yayınevi, İstanbul, 1984, p. 74/80.
[18] Z. Aksu, S. Sen, C.F. Gönen, Continuous fixed bed biosorption of reactive dyes by dried *Rhizopus arrhizus*: determination of column capacity, J. Hazard. Mater. 143 (2007) 362–371.
[19] M.T. Uddin, M. Rukanuzzaman, M.M.R. Khan, M.A. Islam, Adsorption of methylene blue from aqueous solution by jackfruit (Artocarpus heteropyllus) leaf powder: a fixed-bed column study, J. Environ. Manag. 90 (2009) 3443–3450.
[20] R. Hana, Y. Wanga, X. Zhaoc, Y. Wanga, F. Xieb, J. Chengb, M. Tanga, Adsorption of methylene blue by phoenix tree leaf powder in a fixed-bed column: experiments and prediction of breakthrough curves, Desalination 245 (2009) 284–297.
[21] J. Goel, K. Kadirvelu, C. Rajagopal, V.K. Garg, Removal of lead (II) by adsorption using treated granular activated carbon: batch and column studies, J. Hazard. Mater. B125 (2005) 211–220.
[22] M. Asmal, A.H. Khan, S. Ahmad, A. Ahmad, Cole of sawdust in the removal of copper (II) from industrial wastes, Water Res. 32 (10) (1998) 3085–3091.
[23] L. Bernard, P. Bernard, G. Karine, B. Florence, J.P. Croue, Modeling of bromate formation by ozonation of surface waters in drinking water treatment, Water Res. 38 (2004) 2185–2195.
[24] M. Yang, H. Wei, Application of a Neural Network for the prediction of crystallization kinetics, Ind. Eng. Chem. Res. 45 (2006) 70–75.
[25] E. Oguz, A. Tortum, B. Keskinler, Determination of the apparent rate constants of the degradation of humic substances by ozonation and modeling of the removal of humic substances from the aqueous solutions with neural network, J. Hazard. Mater. 157 (2008) 455–463.
[26] E. Oguz, B. Keskinler, A. Tortum, Determination of the apparent ozonation rate constants of 1:2 metal complex dyestuffs and modeling with a neural network, Chem. Eng. J. 141 (2008) 119–129.
[27] S. Kumar, J. Madras, G. Madras, Neural Network Modeling of adsorption equilibria of mixtures in supercritical fluids, Ind. Eng. Chem. Res. 44 (2005) 7038–7041.
[28] A. Sozen, E. Arcaklioglu, M. Ozalp, Estimation of solar potential in Turkey by artificial neural networks using meteorological and geographical data, Energy Conver. Manag. 45 (2004) 3033–3052.
[29] S. Celik, O. Tan, Determination of preconsolidation pressure with artificial neural network, Civil Eng. Environ. Syst. 22 (4) (2005) 217–231.
[30] A. Tortum, The modeling of mode choices of intercity freight transportation with the artificial neural networks and integrated neuro-fuzzy system, Ph.D. Thesis, Atatürk University, 2003, in Turkish.
[31] K.V. Kumar, K. Porkodi, R.L.A. Rondon, F. Rocha, Neural Network Modeling and simulation of the solid/liquid activated carbon adsorption process, Ind. Eng. Chem. Res 47 (2008) 486–490.